Modelling and Evaluation of an Adiabatic Compressed Air Energy Storage System with Packed Beds

Marianne Fjellestad Heitmann Carlos Pfeiffer Elisabet Syverud

Department of Process, Energy and Environmental Technology, University of South-Eastern Norway, Norway,
marianneheitmann94@gmail.com , Carlos.pfeiffer@usn.no , Elisabet.syverud@usn.no

Abstract

Compressed Air Energy Storage (CAES) is a promising alternative for energy storage. An Adiabatic Compressed Air Energy Storage (A-CAES) system has been analysed in this paper, to store excess energy production from a wind turbine generator for up to one week. Compressed air is stored in a cavern of constant volume. The heat produced by the compression of the air during the charge process is stored in several packed beds and used later during discharge to reheat the air prior to energy production.

This paper presents a preliminary thermodynamic analysis estimating the size of the system for a given quantity of energy storage, a dynamic model including packed beds for additional energy storage, and a simulation made in MATLAB to analyse the efficiency of the system. The A-CAES roundtrip efficiency is 53%. The physical limitations of the actual compressors and expanders were taken into account when defining the operational pressures and temperatures in the model. A preliminary capital cost estimation of the system was conducted for Norway, resulting in an estimated investing cost of approximately 2 700 NOK/kWh.

Keywords: compressed air energy storage, adiabatic, thermal energy storage, packed bed, thermodynamic analysis

1 Introduction

The use of renewable energy resources has increased in the past years. In Norway, the energy source that increases the most is wind energy (Øvrebø, 2020). This is an intermittent energy source, so efficient energy storage is needed (Grazzini and Milazzo, 2008). Compressed Air Energy Storage (CAES) Systems are promising for storing energy. In a CAES the excess electrical energy is used to compress air to a high pressure. Then the air is stored in caverns or tanks. When the energy is needed, the pressurized air is released, reheated, and expanded in turbines. The turbines drive a generator that produces electric energy. This energy is then returned to the grid (Eckroad, 2003).

CAES systems typically have a storage capacity of 5MWh – 1GWh, with a discharge time from a couple of hours to days (Moore and Shabani, 2016). In a Diabatic CAES (D-CAES), the air needs to be reheated to produce electric energy. The reheating is done by burning fossil fuels (Calero et al., 2019). This is not a desired solution, because these systems are not CO_2 neutral, and the fuel brings an increase in the operational cost. The Adiabatic CAES (A-CAES) system does not need additional fuel consumption and is the system studied in this work. In this paper, we provide a preliminary thermodynamic analysis estimating the size and cost of an A-CAES for a given quantity of energy storage and using the physical limitations of actual compressors and expanders.

1.1 Adiabatic CAES

In an Adiabatic Compressed Air Energy Storage system (A-CAES), thermal energy storage (TES) replace the combustor of the D-CAES. Energy is expelled as heat during the compression stage. This heat is stored in TES and later used to reheat the air during the expansion stage. This contributes to both higher efficiency of the plant, as well as zero CO_2 emissions from fuel. There has been a lot of research on this type of system but so far only to the stage of simulation of models and theoretical analysis (Yang et al., 2014).

ADELE is a German project where the goal is to build an A-CAES system with a roundtrip efficiency of 70%. When the air is compressed, the heat is captured in a heat-storage facility instead of being released to the surroundings. Later during the discharge, the energy in the heat-storage is released into the compressed air. With this solution, no fuel combustion is needed to heat the air. By avoiding the use of fossil fuel, this technology provides a CO_2 neutral delivery of the peak-load electricity from renewable energy (RWE Power, 2010).

The storage temperature of the plant is one of the most important parameters in an A-CAES. There are three main temperature categories: High temperature A-CAES operates above 400°C, Medium temperature A-CAES runs between 200°C to 400°C, while Low temperature A-CAES operates below 200°C (Degl'Innocenti, 2018). A-CAES simulations using a packed bed as the thermal energy storage component, report an efficiency of 70%, for a temperature range of 30°C to 430°C (Barbour et al., 2015). Wolf and Budt (2014) report a roundtrip efficiency of 52% to 60% for low-temperature A-CAES when the system operates at

temperature from 90°C to 200°C. Sciacovelli et al. (2017) found the roundtrip efficiency to be in the range from 60% to 70% when the TES system has an efficiency of 90% and the system operates at temperatures ranging from 100°C to 500°C.

2 System Overview

The A-CAES presented in this work is a three-stage system that includes compressors, packed beds, turbines, valves, and a cavern, Figure 1.

The cavern is charged by compressed air from the last stage of three compressors. The compressors are powered by surplus energy, e.g. from wind turbines. The hot air out of each compressor enters at the top of the packed bed and exits at the bottom. The packed beds have ceramic Raschig rings that cool down the air and store the thermal energy. The Raschig rings provide a large heat exchange surface allowing quick exchange of heat from the air to the packed bed. The temperature differences across the rings are very low (Heitmann, 2020).

The discharge process is similar, but in reverse order: when the air is released from the cavern, it re-enters the last packed bed, now to reheat the air. In this process, the air enters at the bottom with a lower temperature and exits at the top with a higher temperature due to release of the stored heat from the charge process. The heated air is expanded by a turbine, which drives an AC generator that generates electric energy. The expansion process cools the air, so the air enters the next packed bed to be re-heated. As in the charge process, this happens in three stages, but now the air is expanded in three turbines (one at the discharge of each packed bed). The electric energy generated by the turbines is released back to the grid.

The minimum operational pressure in the cavern is 40 bar, while the maximum pressure is 70 bar. When the pressure is below 70 bar, and there is surplus electric energy, the charge mode is activated. When the pressure in the cavern reaches 70 bar, the compressors stop. The discharge mode starts when the energy is needed. This will go on until there is surplus energy available, or the pressure in the cavern decreases to 40 bar.

Valves are used to control the flow of air, as shown in Figure 1. The check valve makes sure the flow of air only goes in one direction, while the control valves by the cavern regulate the air pressure during the charge and discharge modes. The valve at entry to the first expander keeps the pressure into the expander constant at 40 bar. For the air to flow to the cavern, each increment of air must be compressed to a pressure just above the storage pressure. The valve at the cavern entry ensures that the pressure upstream is always higher than the cavern pressure during the charge mode. A more detailed description of the system can be found in (Heitmann. 2020).

3 Dynamic Model

To analyse the system behaviour we developed a dynamic model based on Heitmann (2020, p. 20). The

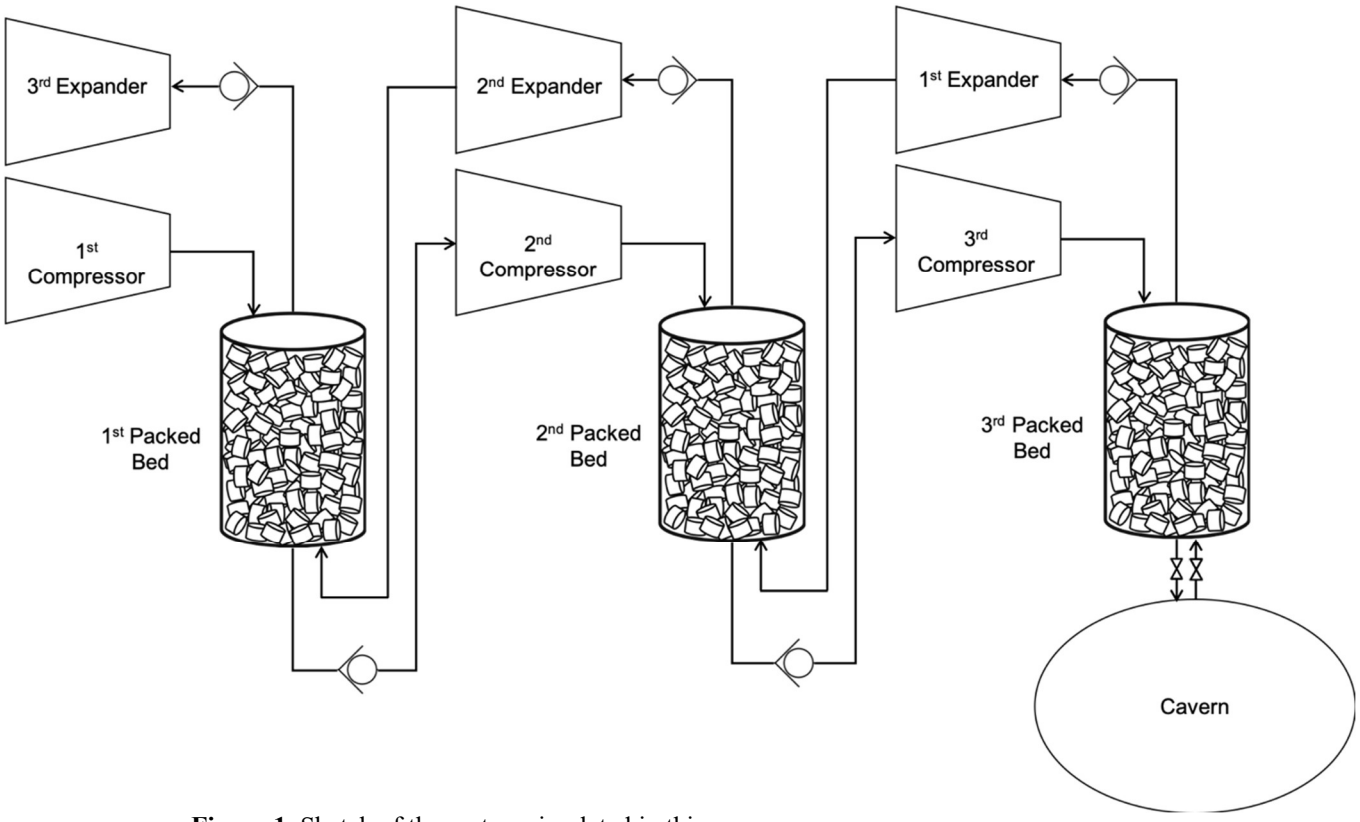

Figure 1. Sketch of the system simulated in this paper

model is described in this section.

3.1 Adiabatic Compression

For an ideal, reversible adiabatic compressor, and assuming ideal gas, the final temperature is given by:

$$T_1 = T_{in}\left(\frac{p_1}{p_{in}}\right)^{\frac{R}{c_p}} \quad (1)$$

where c_p is the specific heat capacity for constant pressure (kJ/kmol K), R is the universal gas constant (8.314 kJ/kmol K), T_1 is the final temperature (K), T_{in} is the temperature of the air into the compressor (K), p_1 is the pressure after compression (kPa), p_{in} is the pressure before the compression (kPa).

The actual work used by the compressor is calculated by Eq.(2):

$$W_{C1} = \dot{m}\, c_p(T_1 - T_{in})\frac{1}{\eta_{isen}} \quad (2)$$

where η_{isen} is the isentropic efficiency of the compressor.

3.2 Packed Bed

The conservation of energy is used to express the equations for the temperature of the air and the solid phase in the packed bed:

$$\Delta E = \dot{m}_{in}\Delta\hat{H} - \dot{m}_{out}\Delta\hat{H} - \hat{h}\, A\,(T_f - T_s) \quad (3)$$

where $\Delta\hat{H}$ is the change in enthalpy (kJ/kmol).
On the right-hand side, the first two terms are the net heat input due to the fluid flow and the last term is the heat transfer to the solid.

The packed bed is used to cool down the air so the temperature of the air will be higher at the top of the bed than the bottom. To make the calculations of the temperature distribution simpler, the bed is divided into n sections. When assuming constant mass flow $\dot{m}_{in} = \dot{m}_{out} = \dot{m}$, the energy rate for the air in a section is:

$$\varepsilon A\rho_a c_{p,a}\frac{dT_a}{dt}\Delta z = -v_a\rho_a A c_{p,a}\frac{dT_a}{dZ}\Delta z - \hat{h}_{vol}A\Delta z\,(T_a - T_s) \quad (4)$$

where, ε is the void fraction of the air, A is the area (m^2), ρ is the density (kg/m^3), $\frac{dT_a}{dt}$ is the change of the temperature of the fluid over time, Δz is the height of the section (m), v is the velocity (m/s), $\frac{dT_a}{dz}$ is the change of temperature of the fluid over the length (K/m), $\hat{h}_{vol}$ is the volumetric heat transfer coefficient (kJ/m^3 s K), and T is the temperature (K). Subscript a stand for air and s for solid. For the solid the energy rate is:

$$(1-\varepsilon)A\Delta z\rho_s c_{p,s}\frac{dT_s}{dt} = -\hat{h}A\Delta z(T_f - T_s) - \varepsilon\, A\frac{d}{dz}\left(\lambda_s\frac{dT_s}{dz}\right) \quad (5)$$

The last term of Eq. (5) is the heat conduction through the solids in the packed bed. The contact between the solids are very small, so this term can be neglected. The equation becomes:

$$(1-\varepsilon)\rho_s c_{p,s}\frac{dT_s}{dt} = -\hat{h}_{vol}(T_f - T_s) \quad (6)$$

To calculate the volumetric heat transfer coefficient, $\hat{h}_{vol}$, between the packing elements (for this work Raschig rings were considered) and the air, the empirical relationship suggested by (Coutier and Farber, 1982) was used:

$$\hat{h}_{vol} = 700\left(\frac{G}{d_p}\right)^{0.76} \quad (7)$$

where G is the core mass velocity of the air (kg/m^{2}s), and d_p are the average particle diameter (m).

3.3 Flow of Air

The flow of air is calculated by: (Heitmann, 2020, p. 22)

$$Q_G = 962\, C_{V\,valve}\sqrt{\frac{p_1^2 - p_2^2}{SG\,T}} \quad (8)$$

where Q_G is the gas flow in standard cubic feet per hour, $C_{V,valve}$ is the coefficient of flow, $p_1$is the inlet pressure in psia, p_2 is the outlet pressure in psia, SG is the specific gravity of the air at 70°F and 14.7 psia, and T Is the absolute temperature in °R. None of these are SI units, so conversion equations are used to get the answer in the correct unit. These kinds of correlations are common to calculate air flow through a control valve, where the value $C_{V,valve}$ can be adjusted by modifying the aperture of the valve to get the required flow.

3.4 Cavern

Since the volume of the cavern is constant, the mass in the cavern will vary due to the pressure increase and decrease over time. The mass balance for the cavern are:

$$\Delta\mathrm{M} = \dot{m}_{in}\Delta t \quad (9)$$

where ΔM is the change in total mass (kg), $\dot{m}_{in}$ is the mass flow of air into the cavern (kg/s), and Δt is the change in time (s). Taking the limit when Δt tends to zero leads to:

$$\frac{dM}{dt} = \dot{m}_{in} \tag{10}$$

The temperature of the cavern will vary as well as the total mass and pressure. The energy balance for the cavern for a small time Δt , neglecting changes in kinetic and potential energy of the air, is given by:

$$\Delta\left(\mathrm{M}\,\widehat{U}\right) = \dot{m}_{in}(t)\widehat{H}_{in}(t)\Delta t \tag{11}$$

Which becomes when Δt tends to zero:

$$\frac{d\left(\mathrm{M}\,\widehat{U}\right)}{dt} = \dot{m}_{in}\widehat{H}_{in}(t) \tag{12}$$

Where:

$$\frac{d\left(\mathrm{M}\,\widehat{U}\right)}{dt} = M\frac{d\widehat{U}}{dt} + \widehat{U}\frac{dM}{dt} \tag{13}$$

$\widehat{U}$ is the internal energy of the air already inside the cavern, and $\widehat{H}_{in}$ is the enthalpy of the air flowing into the cavern. $\widehat{U}$ can be calculated by

$$\widehat{U} = \widehat{U}_0 + c_v(T - T_0) \tag{14}$$

where c_v is the specific heat capacity for constant volume (kJ/kmol K), $\widehat{U}_0$ is a reference internal energy (kJ/kmol) and T_0 is the reference temperature (K). The enthalpy can be calculated by:

$$\widehat{H}_{in} = \widehat{H}_0 + c_p(T_{in} - T_o) \tag{15}$$

where $\widehat{H}_0$ is a reference enthalpy (kJ/kmol) at T_0.

When inserting eq. (17), eq. (18) and eq. (19) into eq. (16), it becomes:

$$M\,C_v\frac{dT}{dt} + \left(\widehat{U}_o + c_v(T - T_0)\right)\dot{m}_{in} = \dot{m}_{in}(\widehat{H}_0 + c_p(T_{in} - T_0) \tag{16}$$

Eq. (20) can be simplified to:

$$\frac{dT}{dt} = \frac{\dot{m}_{in}(c_pT_{in} - c_vT)}{M\,c_v} \tag{17}$$

3.5 Adiabatic Expansion

We use the energy balance for the expander to calculate the temperature of the air after expansion. This is similar to the energy balance for the compressor but since the work is extracted from the system, the work is negative.

For the temperature after the expander, the following equation is used: (Heitmann, 2020, p. 23)

$$T_2 = T_{in}\left(\frac{p_2}{p_{in}}\right)^{\frac{R}{c_p}} \tag{18}$$

The work generated by the expander can be calculated by:

$$W_E = \dot{m}\,c_p(T - T_{in})\,\eta_{isen} \tag{19}$$

where η_{isen} is the isentropic efficiency. Since the expanders are adiabatic, the ideal process is isentropic (Saravanamuttoo et al., 2017).

3.6 Efficiency of the System

The efficiency of the system η is calculated by:

$$\eta = \frac{W_{discharge}}{W_{charge}} \tag{20}$$

where $W_{discharge}$ is the total work produced by the expanders during discharge and W_{charg} is the total work done by the compressors in the charge part.

4 Cost Estimation

To check whether the A-CAES system is economically viable, a cost estimation is needed. A perfect estimation is difficult to accomplish, but a simple estimation for the system based on data from other systems, the given size and the material used is shown in this chapter to give an idea of the magnitude of the cost.

4.1 Compressors and Expanders

We used the SIEMENS DATUM calculator (SIEMENS, 2020) to estimate the cost of the compressors. The DATUM compressors are common in the oil and gas industry. The tool give an initial cost estimates sufficient for preliminary analysis. The tool calculates a three-stage compressor with three impellers and intercooling. The CAPEX of one compressor are assumed to be 500 000 $. According to Buffa et al. (2013) the cost of a Mixed Flow Expander is somewhat the same as for the compressor.

4.2 The Packed Beds

The cost estimation for the packed beds is based on the volume of the column and the mass of the solid.

The height and radius of each column are 30m and 5m, respectively. This leads to a volume of 2 355 m^3. The columns are assumed to be inside the mountain, so the cost of mountain blasting needs to be taking into account. In Norway, mountain blasting is expensive and runs at about 200-300 NOK per cubic meter (NOK/m^3) (Byggestart, 2020).

The solid inside the column are Raschig Rings in ceramic with a void fraction of 74%. The ceramic is Alumina (Al2O3), with a density of 3 900 kg/m^3. The

cost of the ceramic is 1.90 $/kg (19.4 NOK/kg) (Heitmann, 2020).

4.3 The Cavern

The cost of the cavern is the mountain blasting, which is the same as for the packed beds, i.e. 200-300 NOK per cubic meter. The volume of the cavern is calculated to be 41 300 m^2.

4.4 Cost of the System

The total cost of the system is based on the calculation is calculated to be 175 MNOK. With a total capacity of 66 400 kWh, the capital cost estimate is 2 700 NOK/kWh.

This cost estimation only includes the main parts of the system: three compressors, three packed beds, three expanders and a cavern. The cost is the capital cost of the system, not including cost of pipes, valves, or insulation. A substantial amount of money can be saved if an existing cavern is used, instead of blasting one.

5 Simulation and Efficiency Results

5.1 Total Mass in the Cavern

The variations of the total mass in the cavern during the charge and discharge processes are shown in Figure 2 and Figure 3. The red line is the increase of mass in the cavern during the charge process. It starts at an initial mass of 2.03 x10^6 kg, which is calculated by assuming ideal gas at 40 bar and the air cave temperature. After about 30 hours (~108 000 s) the cavern reaches the maximum operational pressure (70 bar) and the maximum mass. When this value is reached the charge process stops.

The blue line shows the decrease of mass in the cavern during the discharge process. It starts at the maximum mass of 3.09 x10^6 kg, and after about 47 hours (~169 000 s) the cavern reaches the minimum operational pressure of 40 bar. The x-axis shows the time in seconds from 0 to 172800 s (48 hours).

5.2 Temperatures over the Packed Beds

The temperature distributions over the packed beds in the charge process are shown in Figure 4. Five sections (n=5) are used in the simulations. Originally, when the system is "loaded" for the first time, all the sections are at the same temperature. The green line shows the temperature of the air in the first section of the packed bed, corresponding to the section where the air enters the packed bed. The purple line shows the temperature of the air in the second section of the bed. The red line shows the temperature of the air in the third section. The pink one shows the temperature of the air in the fourth section. Finally, the turquoise line shows the temperature of the air in the last section of the packed bed. This turquoise line represents the air temperature entering the next compressor stage or the cavern. The black dotted lines represent the temperature of the solid material in the corresponding section, the solid temperature closely follow the air temperature of all sections. The simulation covers 48 hours of operation. The charge process ends after about 30 hours because the cavern is fully loaded with air at 70 bar. This means that the flow of air stops and the temperature of the air and the solid in the packed beds will stop increasing. We assume well-insulated packed beds where the temperatures stay constant when there is no air circulating through the system.

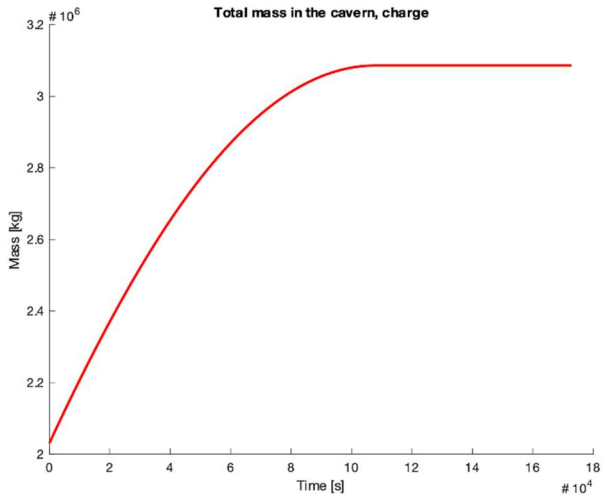

Figure 2. Total mass in the cavern during the charge process.

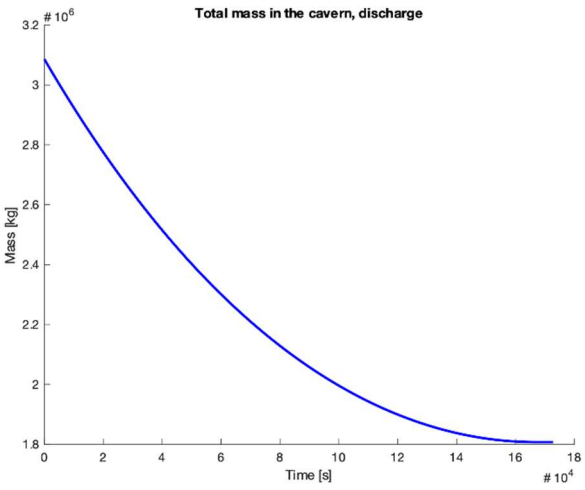

Figure 3. Total mass in the cavern during the discharge process.

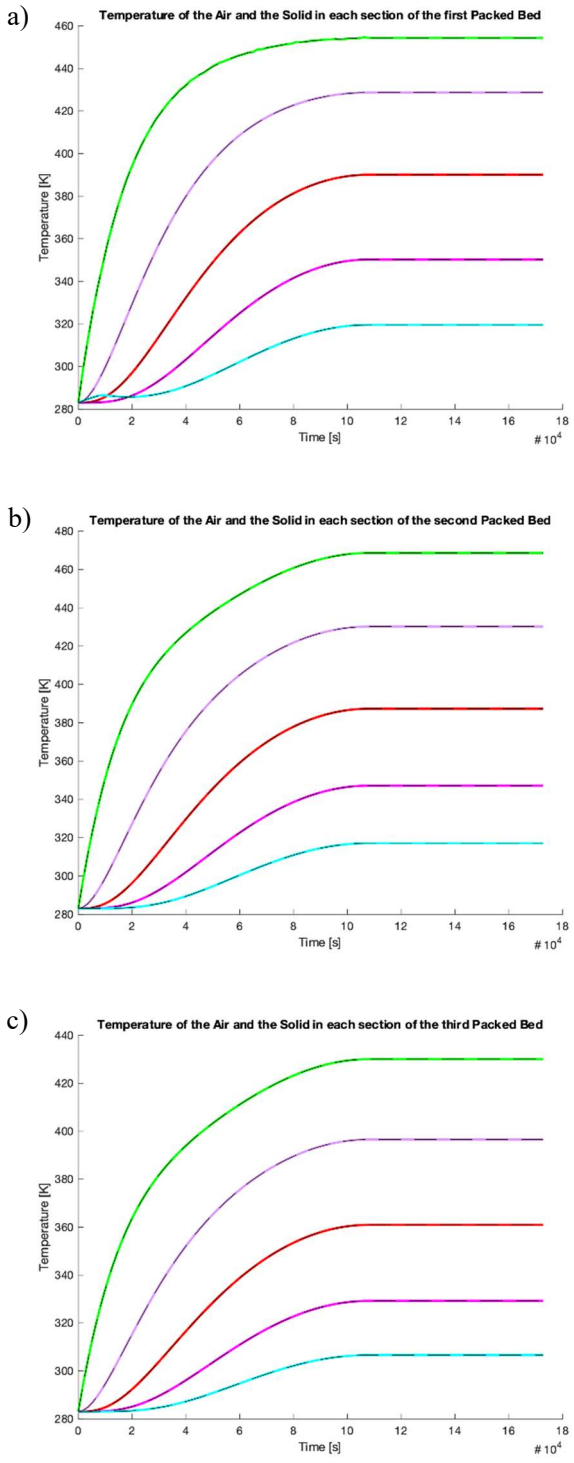

Figure 4. Calculated temperature over the packed beds in the charge process: a) is the first packed bed, b) is the second packed bed, and c) is the third packed bed.

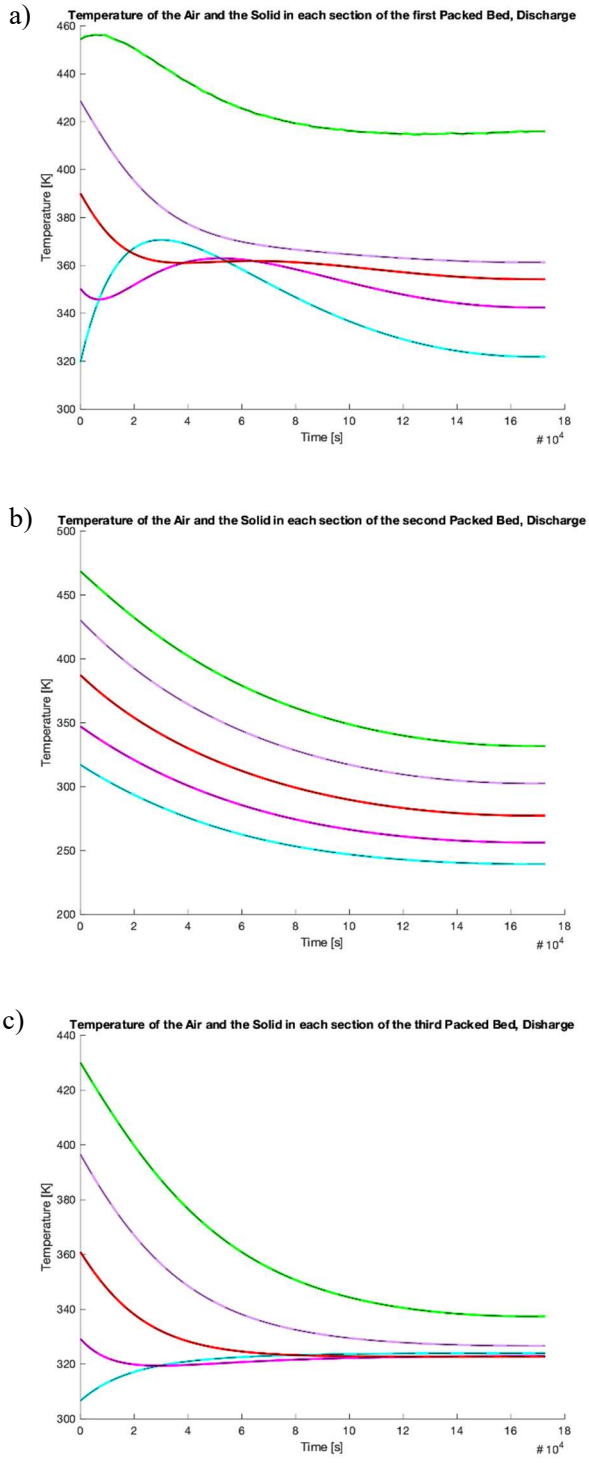

Figure 5. Calculated temperature over the packed beds in the discharge process: a) is the first packed bed, b) is the second packed bed, and c) is the third packed bed.

Figure 5 shows the temperatures over the packed bed during discharge. The initial values for all the sections are the end temperatures reached during the charge process. In the discharge, the first packed bed is the last one from the charge process. The air from the cavern enters at a temperature of 50°C at the bottom of the packed bed and is heated through the bed.

The turquoise line shows the temperature of the air in the bottom of the bed, which is the first section in the discharge process. The pink line shows the temperature of the air in the next section of the bed. The red line shows the temperature of the air in the middle section of the bed. The purple line shows the temperature of the air in the fourth section. Finally, the green line shows the temperature of the air at the top section of the packed bed. This is the air temperature leaving the packed bed and entering the expander. The black dotted lines represent the temperature of the solid in the corresponding section. The solid material temperature closely follows the air temperature in the packed bed.

5.3 System Efficiency

The calculated work done by the three compressors during the charge process was 2 590 kW.

The work produced by the expanders during discharge process was 1 380 kW. This results in an efficiency of 53.4 %. This result indicates that more than half of the electric energy used to compress the air is regenerated in the form of electric energy, without the use of additional fuel to reheat the air.

6 Discussion

The model for the charge process works well and provides realistic results. The air is cooled down to a temperature acceptable for the next compression. The packed bed material is heated fast and reaches the temperature of the compressed air.

The discharge requires operation parameters adjustments to get realistic practical temperatures for the discharge air. According to the simulation, the output temperature for the first expander is between 230 K and 290 K. We consider this temperature range as too low to provide an efficient output from a real turbo expander.

The size of the packed beds was the same in the simulation, but it could be interesting to see how the system would behave if different bed sizes are fitted to the compressors in each stage. Also, the simulation was only done for one type of packing material, ceramic Raschig rings. The system could be tested with other materials, such as metal Raschig rings or marbles to find the solution that provides the highest efficiency with the lowest cost.

In this paper, we have simulated only one cycle (one charge and one discharge). It would be interesting to see how the temperatures over the packed develop with multiple cycles and if the efficiency would be affected.

Although the physical limitations of the components were taken into account, the maximum compressor discharge temperatures are lower than the minimum inlet temperature allowed in most expanders or turbines. This can make it difficult to use existing equipment. For this system to work in reality, special equipment may be needed.

The reviewed literature for similar systems reports an efficiency between 60 - 70 %. Even though the results obtained in our simulations are lower (53.4%), they are similar to the system efficiency of real existing systems using additional fuel to reheat the air is on the range of 40% to 54% (Luo and Wang, 2013). Furthermore, our proposed A-CAES system does not have CO_2 emissions.

The system cost is calculated at 2 700 NOK/kWh. There are not a lot of numbers to compare with. However, in the A-CAES presented by Mignard (2014) the cost is estimated at 334 000 USD/MWh, (3 400 NOK/kWh) in a similar but smaller capacity system using steel as the packing material.

7 Conclusion

We used thermodynamic analysis, modelling, and simulation to make a preliminary estimate of the size of a 12 MW A-CASE system with a storage time of 48 hours. The size of the cavern was calculated to be 41 300 m^3. This value is calculated for a perfect reversible process, so this size is expected to be larger for an actual system.

A dynamic model was created for the system, including the packed beds, the mass and temperature of the cavern, and the work consumed and produced. The model was simulated in MATLAB. We calculated the work done by the compressors as 2 590 kW and the work produced by the expanders as 1 380 kW, which corresponds to a capacity of 66 400 kWh. The system roundtrip efficiency was calculated at 53.4%. The total cost is calculated to be 175 MNOK. With a total capacity of 66 400 kWh, the capital cost estimate is 2 700 NOK/kWh.

We find that the system discharge temperature is too low for use with existing expander technology. In addition, we find that the cost of A-CAES is too high for the system to be economically viable. The cost is site specific and depends on local conditions of the air reservoir and the cavern is by far the most expensive component.

References

E. Barbour, D. Mignard, Y.Ding, and Y. Li. Adiabatic Compressed Air Energy Storage with packed bed thermal energy storage. *Applied energy,* 155: 804-815, 2015. doi:10.1016/j.apenergy.2015.06.019.

F. Buffa, S. Kemble, G. Manfrida, and A. Milazzo. Exergy and Exergoeconomic Model of a Ground-Based CAES

Plant for Peak-Load Energy Production. *Energies, 6*(2):1050-1067, 2013. doi:10.3390/en6021050.

Byggestart. *Graving: Hva koster det? (2020-pris)*. Retrieved from www.byggstart.no/pris/graving. Accessed 8-May-2020.

I. Calero, C.A. Cañizares, and K. Bhattacharya. Compressed Air Energy Storage System Modeling for Power System Studies. *IEEE transactions on power systems*, 34(5): 3359-3371, 2019. doi:10.1109/TPWRS.2019.2901705.

J.P. Coutier and E.A. Farber. Two applications of a numerical approach of heat transfer process within rock beds. *Solar energy,* 29(6):451-462, 1982. doi:10.1016/0038-092X(82)90053-6.

J. Degl'Innocenti. *Compressed air energy storage for clean offshore energy supply*. Norges Teknisk-Naturvitenskapelige Universitet, Master's thesis, 2018.

S. Eckroad, *EPRI-DOE Handbook of Energy Storage for Transmission & Distribution Applications*, Report 1001834, 2003. Retrieved from www.sandia.gov/ess-ssl/publications/ESHB%201001834%20reduced%20size.pdf. Accessed 8-May-2020.

G. Grazzini and A, Milazzo. Thermodynamic analysis of CAES/TES systems for renewable energy plants. *Renewable energy*, 33(9):1998-2006, 2008. doi:10.1016/j.renene.2007.12.003.

M.F. Heitmann. *Modelling and Evaluation of Compressed Air Energy Storage System*. University of South-Eastern Norway, Master's thesis, 2020.

X. Luo and J.Wang. *Overview of Current Development on Compressed Air Energy Storage*. University of Warwick, Coventry, UK, Technical Report, 2013. Retrieved from eera-es.eu/wp-content/uploads/2016/06/Overview-of-Current-Development-on-Compressed-Air-Energy-Storage_EERA-report-20131.pdf. Accessed 8-May-2020.

D. Mignard. Estimating the capital costs of energy storage technologies for levelling the output of renewable energy sources. *International Journal of Environmental Studies: Turbulent Energy*, 71(6):796-803, 2014. doi:10.1080/00207233.2014.967103.

J. Moore and B. Shabani. A Critical Study of Stationary Energy Storage Polices in Australia in an International Context: The Role of Hydrogen and Battery Technologies. *Energies*, 9(9):674, 2016. doi:10.3390/en9090674.

RWE Power AG. *ADELE - Adiabatic Compressed-Air Energy Storage for Electricity Supply*. RWE Power AG, Report, 2010.

H.I.H. Saravanamuttoo, G.F.C. Rogers, H. Cohen, P.V. Straznicky, and A.R. Nix. *Gas turbine theory* (7th ed.), page 59. Upper Saddle River: Pearson. 2017. ISBN: 9781292093093.

A. Sciacovelli, Y. Li, H. Chen, Y. Wu, J. Wang, S. Garvey, and Y. Ding. Dynamic simulation of Adiabatic Compressed Air Energy Storage (A-CAES) plant with integrated thermal storage – Link between components performance and plant performance. *Applied energy*, 185:16-28, 2017. doi:10.1016/j.apenergy.2016.10.058.

SIEMENS. *Datum Calculator*. v LC, F1.1, B1.1, 2020. Retrieved from http://cirs.dresser-rand.com/turbocalc/Index.html. Accessed 4-April-2020.

D. Wolf and M. Budt. LTA-CAES – A low-temperature approach to Adiabatic Compressed Air Energy Storage. *Applied energy*, 125:158-164, 2014. doi:10.1016/j.apenergy.2014.03.013.

K. Yang, Y. Zhang, X. Li, and J. Xu. Theoretical evaluation on the impact of heat exchanger in Advanced Adiabatic Compressed Air Energy Storage system. *Energy Conversion and Management,* 86:1031-1044, 2014. doi:10.1016/j.enconman.2014.06.062.

O.A. Øvrebø. *Opp 43 prosent: Enda en rekord for norsk vindkraft,* 6-March 2020. Retrieved from energiogklima.no/nyhet/datakilder/status-for-vindkraft-i-norge/. Accessed 10-May-2020.